Research article

Roman Danov* and Eugen Thiessen

Development of a high resolution scanning RGB laser headlamp

https://doi.org/10.1515/aot-2020-0045
Received July 15, 2020; accepted September 1, 2020;
published online October 21, 2020

Abstract: Recent rapid progress in automotive lighting technology led to the emergence of headlamps featuring a large variety of light distributions that are highly adapted to provide best possible road illumination in particular traffic situations. Visual assistance systems which highlight relevant objects or project symbols to communicate with other traffic participants, further improve road safety. Implementing all these functions within a single headlamp usually requires the use of several additional modules with high and low resolution. This multitude of modules impacts the installation space, styling and cost of automotive headlamps. This paper presents a high-resolution red-green-blue (RGB) laser headlamp module which provides a good illumination of the road and can also be used for external communication purposes. A specially developed laser scanning unit, based on a bi-axial resonant micro-electro-mechanical systems (MEMS) scanner and a high-power RGB laser, serves as the technical basis. Three module concepts are designed using light simulation, constructed as computer-aided design (CAD) models and integrated into a serial headlamp package. The concepts are based on design, simulation and measurement data of the scanning unit.

Keywords: geometric optical design; illumination design; micro-optical devices; nonspherical mirror surfaces; optical engineering.

1 Introduction

Ever since people started using motorized vehicles on public roads, the contradictory requirements of maximum road illumination and minimum glare for other traffic participants motivated the engineers to develop more sophisticated automotive lighting systems. The simplest headlamp system, defined by the current legislation separates the area in front of the car into two segments with a nearly horizontal cut off line: the high (main) beam on the top and the low (dipped) beam underneath [1]. The driver can decide whether to illuminate the lower part of his field of view with the low beam or activate the high beam to illuminate the upper area, as long as other traffic participants are not glared. The performance of the low beam can be improved by switching on additional light sources or by swiveling the light cone in bends (so called cornering/bending light). In 2010 Volkswagen introduced [2] a headlamp which separated the high beam into two segments with a vertical cut off line. Using the swiveling mechanism of the headlamp, a dark “tunnel” between the left and right headlamp beam could be created and controlled in its width and position: the glare free high beam was born. The recent rapid development of solid state light sources allows separating the driver’s field of view into more and more segments, illuminated by individual light sources (see Figure 1A). First systems [3] implemented a horizontal segmentation of the high beam to illuminate road areas between other traffic participants (see Figure 1B). Later systems [4] also allow a vertical segmentation of the high beam. Light modulation technology from the field of consumer electronics enables high resolution headlamps with millions of pixels, each controlled individually. With this approach light can be modulated in space or in time [5].

Headlamps with a segmented light distribution that offer a high-quality road illumination and enable projections or marking of objects on and next to the road are currently state of the art [7]. High-resolution modules which enable the projection of symbols in color onto the road are the next stage in the headlamp technology development [8]. The projected symbols can be used to assist the driver or to communicate with other traffic participants [9]. The current work aims to develop a single module with high optical efficiency, able to realize all light functions and projections in a broad field of view.

***Corresponding author: Roman Danov**, Volkswagen AG Group Innovation, Wolfsburg, Germany,
E-mail: roman.danov@volkswagen.de
Eugen Thiessen, Volkswagen Osnabrück GmbH, Osnabrück, Germany

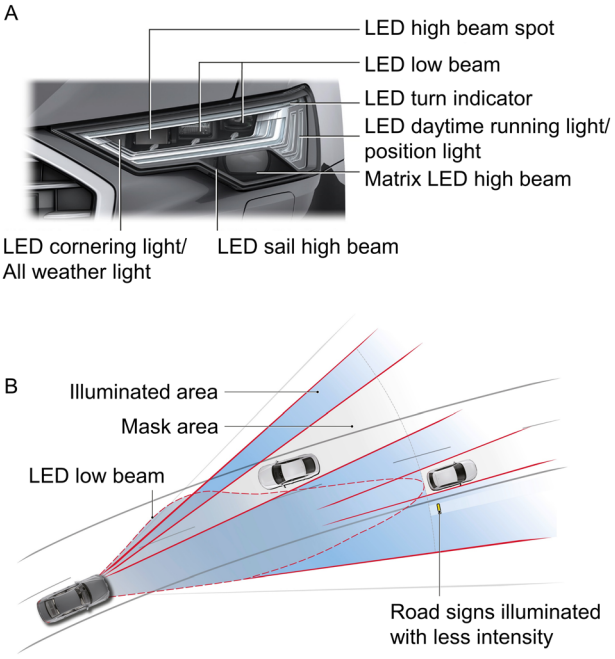

Figure 1: AUDI A6 (model series 2018) headlamp with a segmented glare free high beam A and its schematic pattern of various light functions B [6].

The central component of the high-definition RGB laser headlamp presented in this paper is a so called light engine, which consists of a resonant 2D MEMS scanner (hereafter referred to as MEMS) and an RGB laser light source with collimating optics. The scanning procedure is realized using a small electrically operated mirror that deflects the laser light by means of controlled oscillation around two axes. If the mirror trajectory is known, the power of the RGB laser channels can be modulated in order to produce a desired light intensity and color in defined spatial directions. With a sufficiently high refresh rate, a complete light distribution is achieved that can be dynamically changed. Using redistributing optics the radiation pattern of the light engine can be reshaped. The resulting scanning module combined with an additional foreground base beam module can provide high and low beam light distributions. Furthermore, this setup allows to selectively mask other traffic participants (glare-free high beam) and to project symbols onto the road with a high resolution. The target width of the light distribution of the scanning RGB module is ±15° and the target height ±5°. The maximum light intensity should reach at least 40,000 cd in the direction of the reference axis and follow the current ECE Regulation No. 123 (Economic Commission for Europe) guideline for active lighting functions [10]. The light intensity should decrease towards the edges. By achieving an almost constant light intensity in a broad angular range (±10° horizontal and ±3° vertical), provided a sufficient light flux is available, the concept should be applicable for a purely digital implementation of the bending light function and headlight leveling control [11].

In the following Chapters, the characteristics of the used MEMS are discussed, followed by the characterization of the light engine and the subsequent definition of three modules in an automotive headlamp package. The effect of the MEMS alignment in the module on the achievable resolution is investigated. Lastly, it is demonstrated how the light distribution of the module could look like in order to realize bending light and headlight leveling control without mechanical module movement.

2 Characteristics of the 2D MEMS scanner

A 2D MEMS scanner which has been adapted to the system requirements by Senger et al. from the Fraunhofer Institute for Silicon Technology [12], is used as the basis for the conception and development of a scanning RGB laser headlamp (see Figure 2). During the development of this MEMS, a special focus was put on a relatively large mirror surface (5.5 mm diameter), which oscillates around two perpendicular axes. The amplitudes should be as large as possible and the resonance frequency as high as possible. A vacuum package under a glass lid reduces the air resistance. The scanner is placed at the edge of the printed circuit board (PCB) and the mirror axis with the higher amplitude is positioned perpendicular to this edge. Additionally, the MEMS are equipped with a system, which senses the mirror tilt to trigger the laser modulation according to the desired image. Depending on the mirror position, an algorithm decides which pixel on the rectangular input image (1024 x 512 pixel) the beam is currently corresponding to and switches the laser into a state matching the pixel's luminance and color.

The designed mirror geometry supports two resonant rotational modes (see Figure 3) with the amplitudes $\theta_0^{(x)} = 5°$ (rotation around the x axis) and $\theta_0^{(y)} = 12.5°$ (rotation around the y axis). The MEMS suspension is designed in a way that the axis with the higher amplitude (so-called fast axis) is moved around the axis with the smaller amplitude (so-called slow axis). It is assumed that the mirror oscillates harmonically and that the two modes do not influence each other. More specifically, this means that the mirror tilt around one axis does not affect the mechanical properties (e.g., inertia moment) with respect to the other axis. Under

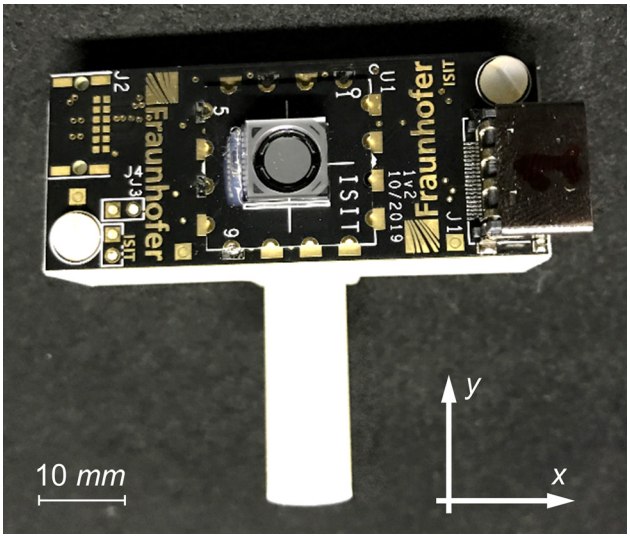

Figure 2: 2D MEMS scanner with a 5.5 mm (in diameter) mirror and vacuum package under a glass lid on the PCB. The target optical scanning angle equals φ(y) target = ±25° and φ(x) target = ±10°.

these conditions, the rotation around each axis can be described as

$$\theta^{(x,y)}(t) = \theta_0^{(x,y)} \cdot \sin\left(f^{(x,y)} \cdot t + \gamma^{(x,y)}\right) \quad (1)$$

with the tilt angle from the equilibrium position θ, amplitude θ_0, oscillation frequency f and phase γ. According to the law of reflection (angle of incidence is equal to the angle of reflection), a laser beam incident perpendicularly to the mirror's equilibrium position, is deflected at an angle equal to twice the mirror tilt angle. Thus, a Lissajous figure with a size of 10° x 25° emerges. However, to ensure that the optics, shaping the incident beam, do not block the deflected beam, the incident beam must be inclined with respect to the wafer. This leads to distortions in the resulting light distribution. These distortions must be characterized for the chosen laser position in order to be able to precisely adjust the downstream optics to the radiation characteristics of the light engine.

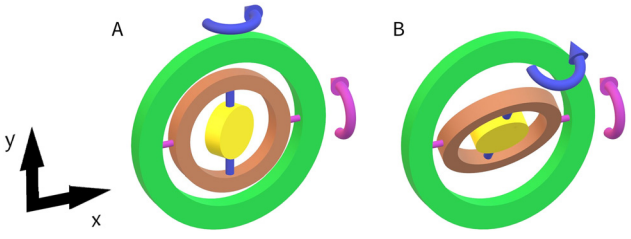

Figure 3: Simplified MEMS model with a mirror (yellow), fast *y* axis (blue), slow *x* axis (magenta) and wafer (green): A rotation mode around the fast axis and B rotation mode around the slow axis.

3 Characterization of the light engine

3.1 Measurement

In order to set up a light simulation for designing the headlamp system, the light distribution of the light engine should be obtained first. Thus, MEMS behavior can be analyzed in terms of light intensity distribution. A test setup comprised of an RGB laser, optical fiber, collimator and MEMS is used for the purpose of this analysis. The RGB laser light with a maximum total power of approximately 9 W from five laser modules (2 x red, 2 x green and 1 x blue) is coupled into a square optical fiber with a core edge length of 100 µm. The optical fiber is connected to an optical holder using a SubMiniature version A (SMA) port. The emitted laser beam is collected by a lens and collimated with a remaining divergence angle of approximately 1° full width at half maximum. The collimated beam is then directed onto the MEMS under an angle of $\alpha_1 = 30°$ to the MEMS normal to avoid a shadowing of the scanning image. The resulting optical axis of the setup is directed towards a photometer head to record the light distribution. The described setup, mounted on an automotive goniophotometer, is depicted in Figure 4.

3.2 Simulation

In parallel to the measurement, a simulation model of the light engine is defined. Simulations are conducted using the non-sequential Monte Carlo ray tracing software LucidShape. The mirror rotation around each axis is assumed according to Equation (1). The probability of the mirror's angular position with respect to one axis is assumed to be independent of the mirror's position or angular velocity relative to the other axis. As a result, the mirror motion can be separated into two independent rotation components: around the fast and around the slow axis. Additionally, to perform a light simulation the mirror motion must be

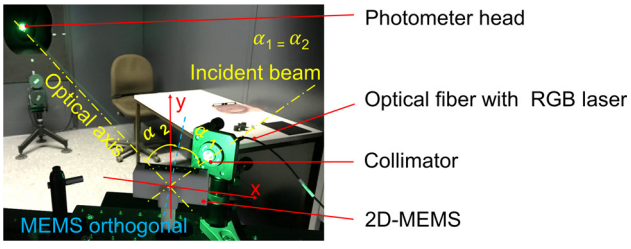

Figure 4: Test setup mounted on an automotive goniophotometer: optical fiber with a coupled RGB laser, collimator optics and MEMS on an adapter plate (from right to left).

discretized. This is achieved by selecting a discrete number of possible mirror tilt values relative to each axis and describing the overall bi-axial movement through a combination of all selected tilts. To reconstruct the mirror motion correctly (see Figure 3), the mirror is first rotated around the fast axis and the resulting geometry is then rotated around the slow axis. The mirror oscillation around the fast axis is divided into 90 temporally equidistant steps:

$$\begin{aligned}\theta^{(y)} &= \left[\theta_1^{(y)}, \theta_2^{(y)}, \ldots, \theta_{90}^{(y)}\right] \\ &= [-12.5°, \ldots, 12.5°]\end{aligned}. \tag{2}$$

Due to their temporal equidistance, each mirror position has an equal probability. On the other hand, the total range of the mirror oscillation is covered by the selected positions. The angle difference between two adjacent mirror states is varying: the difference is small at large deflection angles and largest in proximity of the mirror's equilibrium position as a result of the highest scanning speed. Similarly, the movement around the slow axis is divided in 45 steps:

$$\begin{aligned}\theta^{(x)} &= \left[\theta_1^{(x)}, \theta_2^{(x)}, \ldots, \theta_{45}^{(x)}\right] \\ &= [-5°, \ldots, 5°]\end{aligned}. \tag{3}$$

Out of all combinations of (2) and (3), 4050 mirror positions are obtained which fully cover the oscillation range of the mirror:

$$\left(\theta^{(x)}, \theta^{(y)}\right) = \begin{bmatrix} \left(\theta_1^{(x)}, \theta_1^{(y)}\right), & \left(\theta_1^{(x)}, \theta_2^{(y)}\right), \ldots, \left(\theta_1^{(x)}, \theta_{90}^{(y)}\right) \\ \left(\theta_2^{(x)}, \theta_1^{(y)}\right), & \left(\theta_2^{(x)}, \theta_2^{(y)}\right), \ldots, \left(\theta_2^{(x)}, \theta_{90}^{(y)}\right) \\ & \cdots \\ \left(\theta_{45}^{(x)}, \theta_1^{(y)}\right), & \left(\theta_{45}^{(x)}, \theta_2^{(y)}\right), \ldots, \left(\theta_{45}^{(x)}, \theta_{90}^{(y)}\right) \end{bmatrix}. \tag{4}$$

It can be assumed that for a laser in continuous wave mode, each generated mirror position contributes equally to the light intensity distribution averaged over time. The overall result is therefore achieved by adding up the simulation results of the resulting 4050 states. Since the analyzed structure is symmetric to the plane that is spanned by the MEMS normal and the optical axis, it is sufficient to simulate only half of the states. The other half is obtained through mirroring, thus considerably reducing the simulation time.

3.3 Light intensity distribution of the light engine

The projected light distribution of the light engine is shown in Figure 5A. In addition to the effective scanning image (white page) and a bright spot at its center, sufficiently high laser brightness makes further larger images visible. The white page is the first order image and the main image that is capable of creating an automotive light distribution. Figure 5A also displays the second and third order images. These have a similar shape as the first order image and emerge as a result of multiple reflections between the MEMS mirror surface and the MEMS glas lid. Figure 5B provides an analytical analysis of the light pathways considering Fresnel reflections. The laser beam (100%) is directed at the MEMS. The first Fresnel reflection (4% for reasons of simplification) takes place at the first boundary between glass and air and is visible on the projection screen as a bright spot at HV = 0° (see Figure 6A and B). The remaining light (96%) propagates inside the glass plate. The second boundary between glass and vacuum leads to another Fresnel reflection (again, 4% for reasons of simplification) and contributes also to the spot in the middle of the radiation pattern. Any further Fresnel reflections of this beam portion within the glas lid can be ignored. Though the zero order image (no interaction with the mirror surface) contains only 8% of the total light flux, it is distributed across a solid angle that is approximately two magnitudes smaller than that of the main image. Consequently, the light intensity of the zero order reflection is relatively high. The remaining light flux of 92% is reflected (with reflection losses) by the mirror back to the glass plate with a deflection equivalent to the double of the mirror tilt. Additional Fresnel reflections at boundary surfaces emerge during the second transition through the lid, reflecting light back onto the mirror. The first order image (light which has interacted with the mirror surface once) consequently has a 72% share of the total light flux provided by the laser. Accordingly, the projected second order image (two reflections on the mirror surface) has a light flux share of less than 5%. Furthermore, the expanse of the second image reaches twice the expanse of the first image in each dimension due to additional deflection of light caused by the second reflection from the mirror. Thus, the light intensity of the second order image is approximately two magnitudes lower than the light intensity of the first order image. The third order image with a light flux share far below 1% can be ignored due to a very low intensity: In both directions, the aperture angle of the third order image is three times as large as the aperture angle of the first order image. In the area of the first order image, all images overlap. Therefore, it is impossible to use only the main image ignoring other reflection orders. Hence, further measures must be taken to reduce the described ghost images in the next MEMS generation to fulfill strict stray light and glare requirements for automotive light distributions with this system.

The light engine radiation pattern is obtained using a goniophotometer (as described above and displayed in Figure 4) within an angular range of $h = \pm 25°$ and $v = \pm 9°$ with a resolution of $\delta h = 0.1°$ and $\delta v = 2°$. Figure 6A shows the measured light distribution. The illuminated area has a quadrilateral, but not exactly rectangular shape. There is a step visible in its lower edge. This effect can be explained by the vertical resolution and the adjustment of the system: the upper edge of the light distribution serves as reference for the horizontal alignment, the lower edge is therefore slanted. Hence, the lower edge of the light distribution traverses a scanning line of the goniophotometer and an impression of a step appears. The corners of the light distribution exhibit a significantly higher intensity compared to the central area. The reason for this is a longer dwell time of the scanning laser beam spot at the turning points at the edges of the light distribution. Moreover, a peak with the maximum intensity is observed at HV = 0. The intensity of this peak is approximately two orders of magnitude higher than the intensity in the remaining image. The measurement shows a scanning angle of $\varphi^{(y)}_{\text{actual}} = \pm 23°$ and $\varphi^{(x)}_{\text{actual}} = \pm 8°$. A minor deviation from the target values ($\varphi^{(y)}_{\text{target}} = \pm 25°$ and $\varphi^{(x)}_{\text{target}} = \pm 10°$) can be explained by a certain tolerance towards the specifications during mirror manufacturing and should be adjusted in the next MEMS generation.

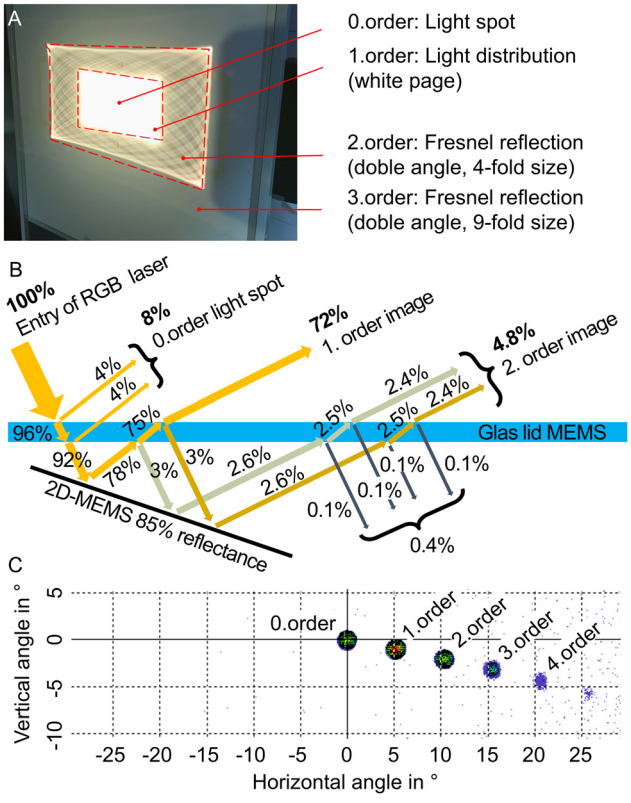

Figure 5: Qualitative analysis of the light engine's light intensity distribution: A Illumination of a projection screen and definition of the order of each emerging image, B calculation of the relative share of single reflections and transmissions in reference to the total light flux, C simulation of the various orders of a pixel.

The light simulation of the measured setup is presented in Figure 6 B. The resulting light distribution is vertically symmetric. Due to the non – perpendicular MEMS irradiation (see arrangement in Figure 4), the right edge of the light distribution is longer than the left one. This causes the light distribution to be horizontally slightly asymmetric, which confirms the measurement results. The analysis of the geometry shows that the longer vertical edge of the light intensity distribution is formed when the mirror is tilted around the y axis towards the laser. This situation represents an almost perpendicular incidence of light on the mirror surface (for the equilibrium state of the oscillation around the x axis) and the vertical deflection of the laser beam equals almost double the mechanical mirror displacement around the slow axis. As the mirror surface tilts further away from the laser around the y axis, the laser beam hits the surface in a steeper angle of incidence causing the deflection around x to be less than double the mirror displacement around the corresponding axis-which is the case for the shorter left edge of the light intensity distribution. Simulations further show that the horizontal expansion of the light distribution (in the plane spanned by the incident beam and the MEMS normal) matches the expected $\varphi^{(y)}_{\text{target}} = \pm 25°$ (double the mechanical mirror displacement). Figure 6D depicts the sections of the light distributions. The behavior of the measured curves is in good agreement with the simulated light distribution. Deviations emerge at the edges and in the area of Fresnel reflections because large gradients cannot always be accurately depicted in a measurement due to the finite sensor size. Subsequently, a simulation without an encapsulation of the MEMS is conducted to emulate the planned MEMS optimization aiming at minimizing the ghost images. Figure 6C shows that the light spot in HV = 0° disappears completely while the utilized light flux increases. The scanning angles remain the same. This model serves as a basis for the design and construction of the module concepts.

4 Conceptualization of a scanning RGB laser headlamp

The results of the light engine characterization are used to design an automotive headlamp module. It is hereby assumed that the module is to be integrated into the

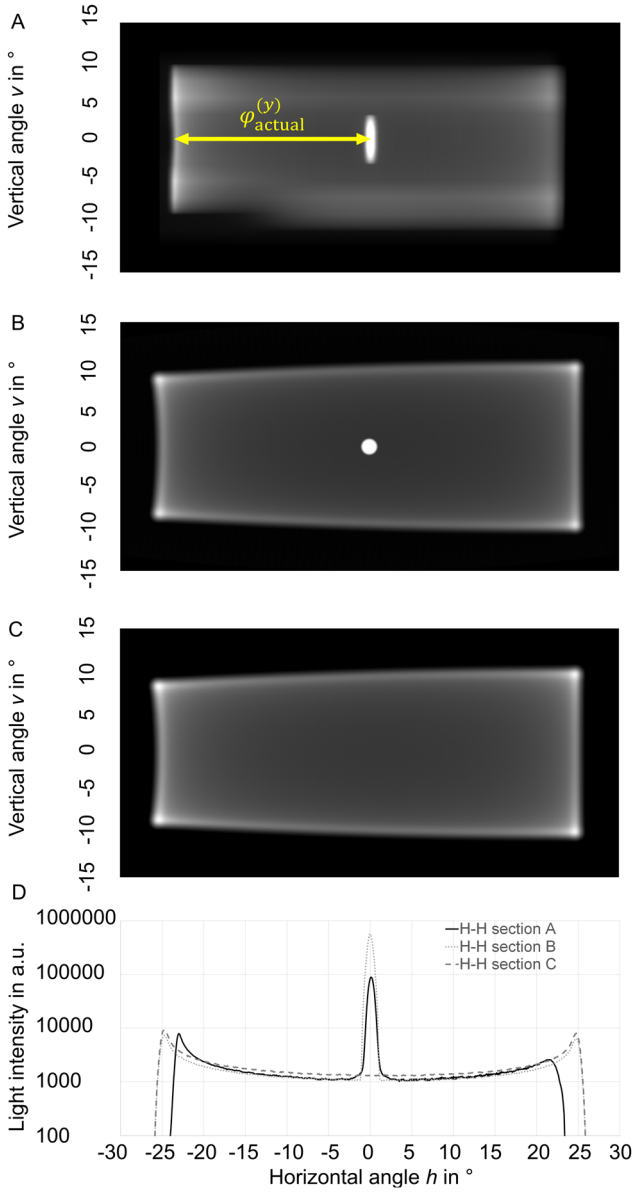

Figure 6: Light distribution of the light engine: A measured using an automotive goniophotometer, B simulation with glass lid, C simulation without glass lid, D sections through A, B and C at v = 0°.

headlamp of a Volkswagen Tiguan. The CAD data is analyzed and the available installation space is defined. The most important dimension is the distance between the outer lens and the rear housing wall. This distance equals to approx. 240 mm (see Figure 7).

Though masking specific areas and symbol projection can be performed using the light engine directly [13], the aperture angle and the locations of the maxima in its radiation pattern are not suitable for an automotive light distribution. These attributes must be reshaped using secondary optics. However, the secondary optics should only distort the Lissajous scan trajectories of the light engine, not interrupt them. Otherwise the adjustment and controlling effort would significantly increase. To avoid chromatic effects, a redistributing reflector is used instead of a lens or other transmitting optical components. The redistributing reflector is placed at the rear housing wall of the headlamp, where the serial BiLED module is usually positioned. This reflector is illuminated by the light engine which is located off the resulting optical axis. It deflects the light in the direction of travel. Within the housing, the light engine can be positioned either beneath the redistributing reflector or next to it inboard. The latter option must be discarded as it would interfere with the planned

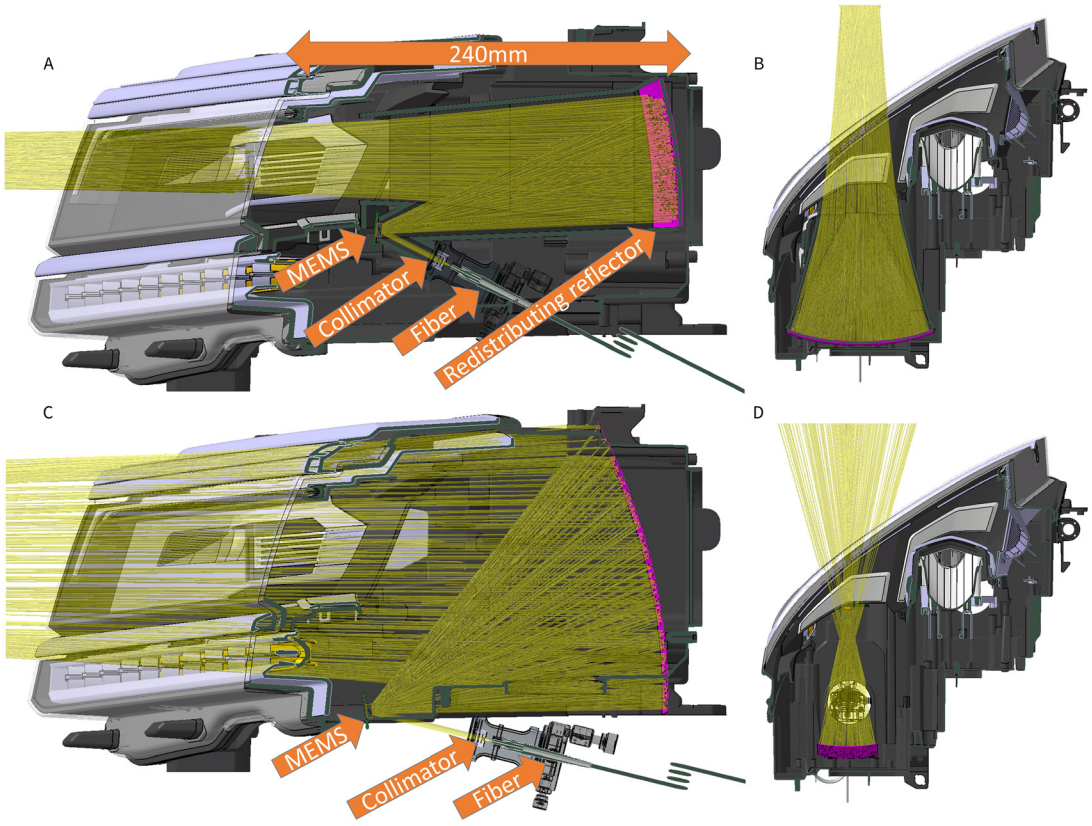

Figure 7: Module concept with redistributing reflector and light cone inside a serial headlamp: A and B arranged horizontally (vertical fast MEMS axis) and C and D arranged vertically (horizontal fast MEMS axis).

foreground module. Therefore, the orientation of the MEMS is the only degree of freedom in the design left: the fast axis can be positioned horizontally or vertically. This axis defines the direction of the higher resolution of the light engine [14] and the larger dimension of the redistributing reflector. In the present work, both orientation options are implemented, integrated into the headlamp package and analyzed. The results are depicted in Figure 8. The horizontally elongated shape of the redistributing reflector allows a compact light emitting area in vertical direction and the light cone can be good integrated into the existing headlamp design. The concept with the vertically elongated redistributing reflector requires the entire height of the outer lens for the light cone of the module. However, a higher vertical resolution is expected as a result of the orientation of the light engine – an advantage for the symbol projection [15]. The light distribution (white page) of both modules can be compared in Figure 8A and B. The efficiencies as well as the light intensity distributions of both modules are very similar. The minor differences are caused by numerical variations in the calculation of the reflector shape. The light intensity peaks in the center of the light distribution, near HV = 0°. It decreases towards the edges in all directions. If necessary, the exact pattern can be further adapted via additional iterations in the reflector layout: The light intensity can decrease slower or a constant intensity area can be implemented.

The resolution dependence on the orientation of the fast MEMS axis is analyzed. For this purpose, selected pixels at approx. h = {–15, –10, –5, 0, 5, 10, 15} and v = {–5, –2, 0, 2, 5} are simulated, displayed and compared. Figure 8C and D shows that the pixel size increases towards the edges of the light intensity distribution for both setups. The module with the horizontal fast axis has smaller vertical pixel dimensions and can therefore resolve more accurate in this direction. The module with the vertical fast axis can resolve finer details in the horizontal direction. An analysis of the headlamp package shows, that the horizontally elongated redistributing reflector fits better into the headlamp package and delivers a pixel size at the center of the light distribution comparable to that of the vertically elongated redistributing reflector. For that reason, this concept was chosen for the final module development inside the headlamp housing. The results are shown in Figure 9. All module components are integrated into the available package. Both the redistributing reflector

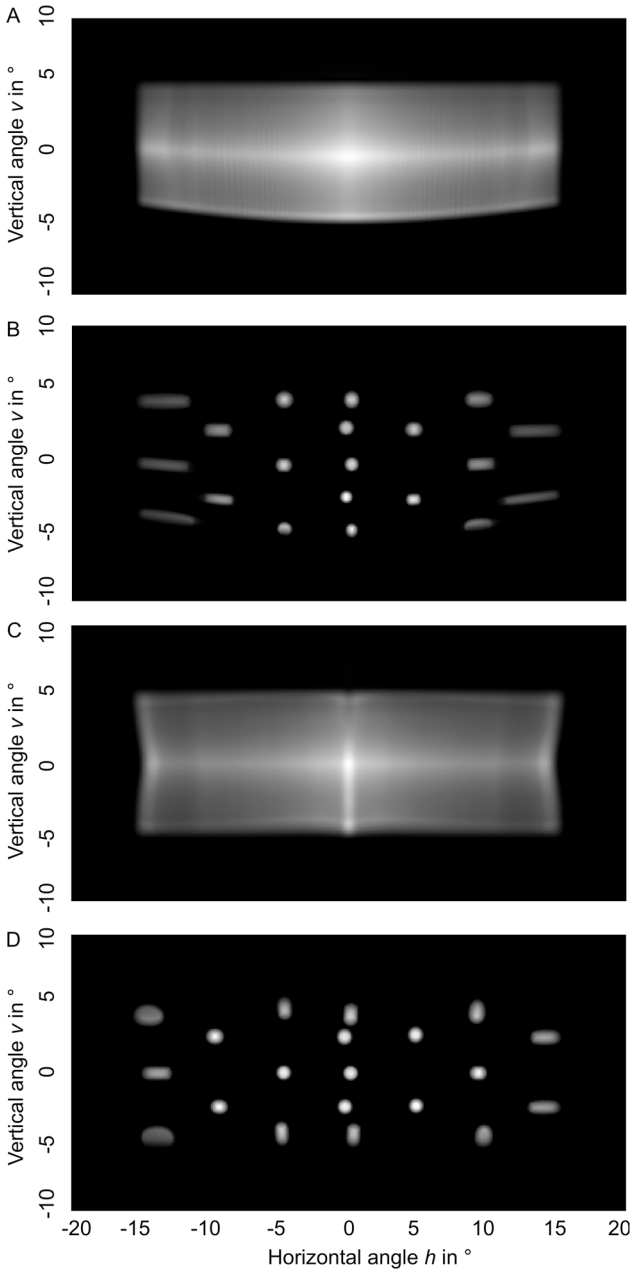

Figure 8: A comparison of the light intensity distributions and resolutions of two modules with different orientations of the fast MEMS axis: A white page and C selected pixels of the module with a horizontally oriented fast axis and B and D of the module with a vertically oriented fast axis, respectively.

and the black tube body that encloses the light cone can be produced via plastic-injection molding. Obviously, bezels and housing have to be slightly modified compared to the serial design. However, the light cone exits the headlamp without being shaded.

To visualize a possible evolution of the developed module, the redistributing reflector depicted in Figure 9 has been adapted in order to produce a light intensity

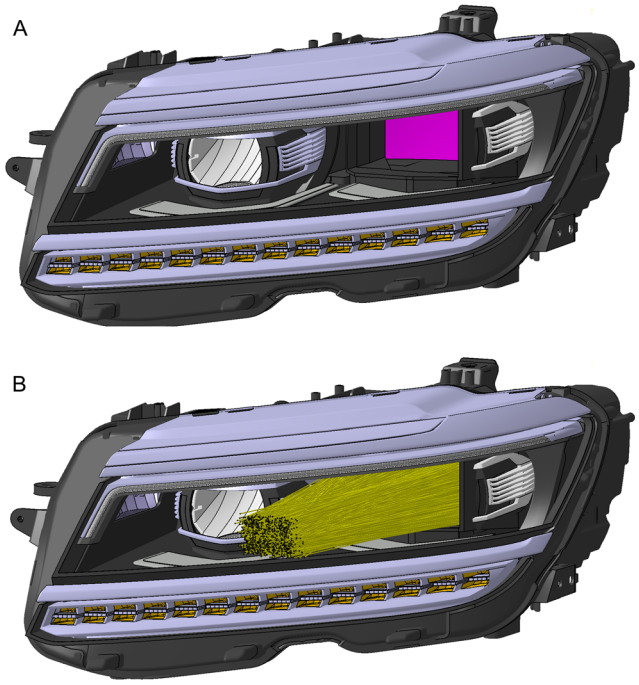

Figure 9: Serial headlamp of a Volkswagen Tiguan with integrated scanning module based on 2D MEMS with a vertical fast axis and its light cone (yellow).

distribution following in its horizontal section the curve depicted in Figure 10A. The shown light intensity flat top should also be realized in vertical direction within the angle range of ±3°. Figure 10B and C show the resulting light distribution: the desired profile is mostly matched. Such a white page allows the peak of the light distribution to be shifted electronically in a broad angle range without loss of maximum intensity, solely by modulating the laser. The module can therefore be statically installed inside the headlamp. The displacement resolution of such a system is approx. 0.02° and is only limited by the control electronics. The marking resolution in the central area of the light distribution is less than 1° (see pixel size in Figure 10D). The masking resolution is comparable with the displacement resolution and is far below 1°. The luminous flux of approx. 1000 lm currently provided by the laser is yet insufficient for an electronic headlamp leveling. It needs to be increased to more than 4000 lm in order to realize a cornering light function and leveling control without mechanical swiveling and still achieve a sufficient maximum light intensity.

5 Summary

The paper presents the development process of an RGB laser headlamp on the basis of a resonant mirror oscillating

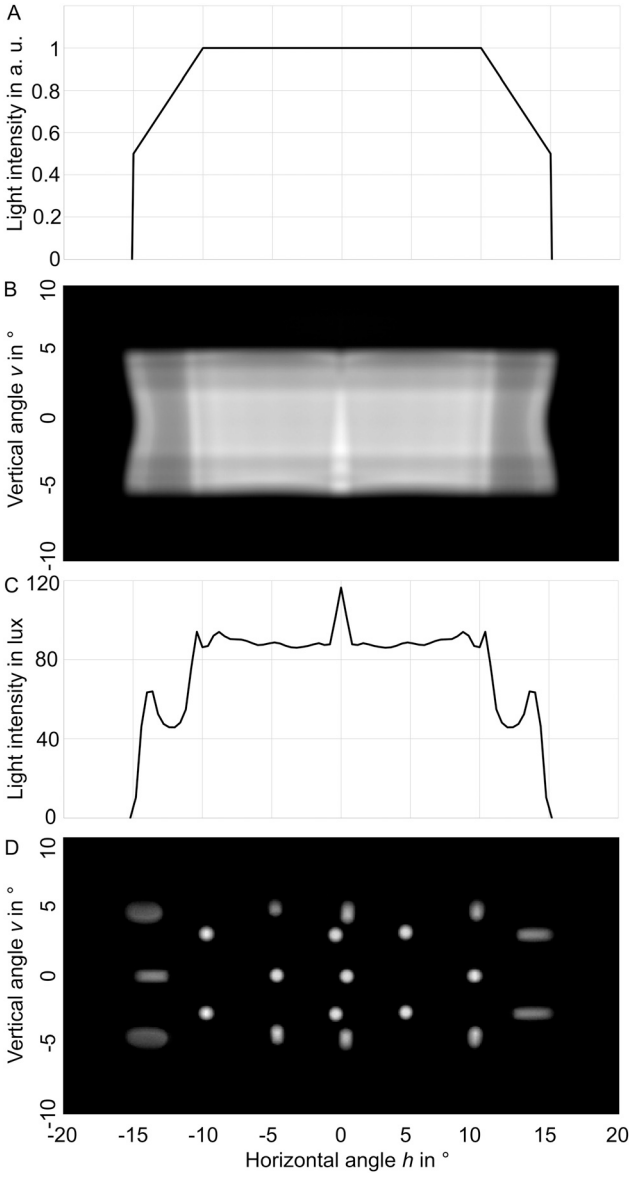

Figure 10: Light distribution of a module which allows an electronic maximum shifting: A horizontal section (v = 0) through the desired light intensity distribution, B the result of the optical design, C horizontal section (v = 0) through the achieved light intensity distribution and D selected pixel for visualizing the module resolution.

around two axes. A MEMS scanner was developed and produced according to defined requirements. It serves as the core part of a high resolution module which allows the projection of symbols in any combination of red, green and blue onto the road. In combination with a foreground module, a headlamp, equipped with this technology, can provide adaptive low beam, glare-free high beam and marking beam functions. Assuming a sufficiently strong light source, the concept can be further extended to generate a fully adaptive light distribution in a broad angle range and simultaneously enable functions that require very fine-grained cut-off shifts (e.g., headlamp leveling control, bending light, etc.) without mechanically moving parts. During the development, the light engine comprised of the MEMS and the laser light source was photometrically characterized by goniophotometer measurements and with the aid of a simulation method specially developed for this purpose. Based on the knowledge gained, a CAD model of the module was designed and integrated into a serial automotive headlamp package. It was demonstrated that the orientation of the MEMS axis with the higher amplitude has a significant impact on the module resolution. The presented system offers the advantage of a high frame rate resonant scanner. By means of a redistributing reflector it eliminates its downside: high intensity towards the edges of the radiation pattern. The individual layout of the redistributing reflector allows a high flexibility in the light distribution design in terms of cross section and aperture angle without changes in the module core component, the light engine. A low number of optical components and their simplicity allows a broad application in multiple vehicle models and classes. As the next step towards serial production, additional tests under realistic automotive conditions in real driving situations must be conducted. Furthermore, a strategy for the generation of the light distributions and symbols needs to be developed.

An alternative application of the presented optical approach is a LIDAR system, which can support autonomous driving systems. The LIDAR approach suggests implementing an infrared light source into the headlamp module and using the already existent MEMS and redistributing reflector to sample the vehicle's surroundings. Alternatively, a separate LIDAR system can be designed with a dedicated redistribution of the scanning velocity and field of view. Further possible applications are optical lithography and imaging.

Acknowledgment: This research has been funded by the Federal Ministry of Education and Research of Germany in the framework of "Mensch – Technik – Interaktion" for project "Kooperativer Laserscheinwerfer – KoLa" (project number 16SV7615). The authors want to also send special thanks to our cooperation partner "Fraunhofer for Silicon Technology (ISIT)".

Author contribution: All the authors have accepted responsibility for the entire content of this submitted manuscript and approved submission.

Research funding: None declared.

Conflict of interest statement: The authors declare no conflicts of interest regarding this article.

References

[1] Regulation No 48 of the Economic Commission for Europe of the United Nations (UNECE) - Uniform Provisions concerning the Approval of vehicles with regard to the installation of lighting and light-signalling devices, 2019/57, 16.01.2018.

[2] C. Amsel, G. Florissen, and S. Pietzonka, *Die Nächste Generation Lichtbasierter Fahrerassistenzsysteme, ATZ – Automobiltechnische Zeitschrift*, Springer Automotive Media: München, 2010, pp. 758–763, ISSN0001-2785, Ausgabe 10/2010.

[3] M. Hamm, "Safety improvement generated by pioneering new matrix and direction indicator functionalities," in *Proc. of the 10th International Symposium on Automotive Lighting (ISAL)*, vol. 15, Darmstadt, Germany: Utz Verlag Gmbh, pp. 319–329, 2013.

[4] M. Maier, J. Moisel, and F. Herold, *Multibeam-Scheinwerfer in der Mercedes-Benz CLS-Klasse, ATZ – Automobiltechnische Zeitschrift*, Wiesbaden: Springer Fachmedien Wiesbaden, ISSN: 0001–2785, Ausgabe 2/2015, vol. 117, pp. 16–21, 2015.

[5] C. Gut, *Laserbasierte hochauflösende Pixelsysteme, Dissertation*, Karlsruhe, Germany, Karlsruher Instituts für Technologie, 2017.

[6] Audi A6, model series 2018, Original images adapted to paper context, Copyright AUDI AG, Retrieved from: www.audi-mediacenter.com/de/audi-a6-39 on 14 09 2020.

[7] W. Huhn, S. Berlitz, M. Hamm, and S. Omerbegovic, *Digitales Licht: von der Matrix zum Mikrospiegel, ATZ Automobiltech*, München: Springer Automotive Media, vol. 120, pp. 19–25, 2018.

[8] R. Danov and J. Roth, *Scannender RGB-Laserscheinwerfer*, Davos, Switzerland, Lichttechnische Konferenz LICHT2018, 2018.

[9] M. Powelleit, S. Winkler, and M. Vollrath, "Lichtbasierte Kommunikationskonzepte zur Unterstützung von Kooperation im Straßenverkehr", Conference: 3. *Kongress Fachgruppe Verkehrspsychologie* (Poster), 2019, https://doi.org/10.13140/RG.2.2.27424.64007, Saarbrücken, Germany.

[10] Regulation No. 123 of the Economic Commission for Europe of the United Nations (UN/ECE) - Uniform Provisions concerning the Approval of Adaptive front-lighting systems (AFS) for motor vehicles, 2019/273, 10.02.2018.

[11] E. Tatartschuk and R. Kreuzer, *Laserbasiertes scannendes Pixellicht: Rotatorischer Spiegelansatz, Optische Technologien in der Fahrzeugtechnik: 7*, Karlsruhe, Germany, VDI-Tagung, 2016, pp. 269–280.

[12] F. Senger, J. Albers, U. Hofmann, et al., *A Bi-Axial Vacuum-Packaged Piezoelectric MEMS Mirror for Smart Headlights*, San Francisco, California, USA, Proc. SPIE 11293, MOEMS & Miniaturized Systems XIX, 1129305, 2020, https://doi.org/10.1117/12.2542802.

[13] J. Roth, *Untersuchung von elektrodynamischen Microscannern zur Darstellung von Lichtssymbolen in der Kraftfahrzeugbeleuchtung*, Hannover, Germany, Dissertation, Leibniz Universität Hannover, 2016.

[14] U. Hofmann, *Entwicklung eines mikromechanischen Strahlablenksystems für Laser-Projektions-Displays*, Itzehoe, Germany, Dissertation, Christian-Albrechts-Universität zu Kiel, 2015, 978-3-7392-0919-7.

[15] R. Danov and E. Thiessen, *Projektionen mit einem scannenden RGB-Laserscheinwerfer, lichttechnische Konferenz LuxJunior2019*, Germany, Dörnfeld/Ilm, 2019.

Bionotes

Roman Danov
Volkswagen AG Group Innovation, Wolfsburg, Germany
roman.danov@volkswagen.de

CV Roman Danov

Project manager at Volkswagen AG Group Innovation, Department Light & Displays	Since 2017
Project manager for automotive lighting EDAG Engineering GmbH in Wolfsburg/Germany	2015–2016
Scientist at the Institute of Product Development, Department Optomechatronic Systems/Leibniz Universität Hannover	2012–2015
Bachelor and Master of Science in Mechatronics at the Leibniz Universität Hannover	2005–2012

Eugen Thiessen
Volkswagen Osnabrück GmbH, Osnabrück, Germany

CV Dr. Eugen Thiessen

Specialist for optical technologies at Volkswagen Osnabrück GmbH	Since 2016
Specialist for optical technologies at Bertrandt Cologne GmbH	2011–2016
Researcher at Department of Materials Science and Engineering in Clemson University, SC.	2010–2011
Dr. rer. nat. at Friedrich Alexander University of Erlangen-Nuremberg (School in Advanced Optical Technologies)	2008–2010
Diploma in physics at Osnabrück University	2003–2007